F-16 Assignment

AE4301P
Automatic Flight Control System Practical

Martijn Brummelhuis - 4442164
Mayukh Sarkar - 5219507
Nick Pauly - 4550447

Design of pitch rate command and landing (glideslope and flare) systems based on the 2003 non-linear F16 model by R.S. Russell. Assignment and report to specification of the course AE4301P of Delft University of Technology, faculty of Aerospace Engineering.

TU Delft

F-16 Assignment

AE4301P
Automatic Flight Control System Practical

by

Martijn Brummelhuis - 4442164
Mayukh Sarkar - 5219507
Nick Pauly - 4550447

in partial completion of the degree Master of Science
at the Delft University of Technology,
faculty of Aerospace Engineering,
department Control & Simulation

Deadline	February 7, 2021
Course responsible	Dr.ir. E. van Kampen
Course instructors	Dr.ir. E.J.J. Smeur
	Dr.A. Jamshidnejad

TU Delft

Preface

Preface…

Martijn Brummelhuis - 4442164
Mayukh Sarkar - 5219507
Nick Pauly - 4550447
Delft, February 2021

Contents

1

Introduction

2

Trim and Linearisation

In this chapter the preparation for the flight controller design is elaborated upon. First, the flight condition is determined and explained. In the next section, the model will be extended and linearised for use. The last section contains an analysis of the open-loop system to get insight into the default behaviour of the F16.

2.1. Flight condition

Design of controllers cannot simply be done once for one flight condition and be expected to work in any situation. In principle, the controller should be redesigned for different flight conditions, and for example gain scheduling can be used to switch between appropriate controllers when the aircraft is in a specific flight condition.

For the scope of this assignment, only two flight conditions are considered and they are stated in Table 2.1.

	Altitude [ft]	**Airspeed [ft/s]**	**Condition**
Accelerometer	15000	500	Straight, wings level (1)
Controller design	20000	600	Straight, wings level (1)

Table 2.1: Flight conditions used

2.2. Trim and linearisation

Before we can proceed with analysis and design of controllers, the model needs to be trimmed and linearised (in this order). Trimming is essential because it means determining the inputs for which the aircraft is in equilibrium for the given flight conditions.

Linearisation can only happen around a certain point (because the linearisation approximations are only valid close to the linearisation point), which is the equilibrium point determined by the trimming procedure. The analysis and subsequently designed controller then depend on this linearisation and cannot be expected to function adequately when the actual flight conditions deviate too much from those off the linearisation or trim point.

2.2.1. The trim and linearisation procedure

To do this trim and linearisation for the F16 model accompanying this assignment, the file `FindF16Dynamics` should be run. The running file asks for the flight conditions, which are inputted as given in Table 2.1. The `FindF16Dynamics` script uses the `TrimF16` script to minimise a cost functionRussell, 2003 related to how well the aircraft is trimmed. The results of the cost functions are displayed in Table 2.2, to show that the optimisation approximates 0 close enough to be used for the analysis presented in this report.

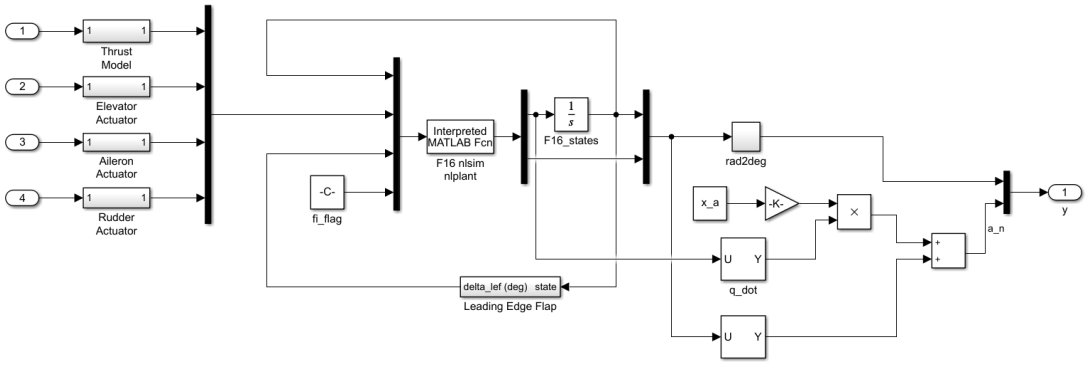

Figure 2.1: Modified Simulink model to include a_n

Accelerometer		Controller design	
High-Fi	Low-Fi	High-Fi	Low-Fi
7.1856e-06	4.2881e-29		4.9829E-29

Table 2.2: Values for the cost function after minimisation

2.3. Accelerometer position

Before we start the open-loop analysis, we look at the influence of the accelerometer positioning. As explained in the manual (van Kampen, 2020), placing the accelerometer close to the pilot can be used to precisely control the g-loads on the pilot, and this sensor input can also be used to steady the aircraft in case of the pilot passing out (due to high g-loads).
The normal acceleration at a point x_a along the X_b axis (forward of the aircraft c.g. positive) is given by Equation 2.1. The derivation for this is given in the manual.

$$a_n = \frac{-(n_z - \dot{q}x_a)}{g_D} = n_z + \frac{\dot{q}x_a}{g_D} \tag{2.1}$$

The Simulink model `LIN_F16Block` is now modified to accommodate a_n as a 19^{th} entry in the output equation. This modification is shown in Figure 2.1. After running the `FindF16Dynamics`, the new state-space matrices can be found. The equation for the new output entry a_n is then Equation 2.2 (coefficients are given by the last rows of matrix C and D). The states that a_n is dependent on are the ones with a non-zero coefficient. These are given in Table 3.1

$$a_n = -3.2432*10^{-5}*h - 9.6797*10^{-6}*\theta + 4.0*10^{-3}*V + 9.9298*\alpha + 0.9664*q + 2.08*10^{-2}*n_y \tag{2.2}$$

Symbol	State name
h	Altitude
θ	Pitch angle
V	Airspeed
α	Angle of attack
q	Pitch rate
n_y	Lateral load factor

Table 2.3: States on which a_n is dependent

The elevator-to-normal-acceleration transfer function can then be found by using the transfer function command on the low-fidelity state space model (command `tf(SS_lo)`) and taking the transfer function of the second input and 19^{th} output. Pole-zero cancellation is realised by means of the `minreal()` command. The transfer function output is given in Equation 2.3.

$$\frac{a_n}{\delta_e} = \frac{0.4210s^4 - 1.84s^3 - 22.1497s^2 + 0.077s + 0.0012}{s^5 + 21.7321s^4 + 33.0006s^3 41.4799s^2 + 0.5546s + 0.2930} \tag{2.3}$$

From this transfer function, a step response can be obtained. For this analysis, we will use a negative step input (elevator deflected upwards), which results in the responses given in Figure 2.2 and 2.3.

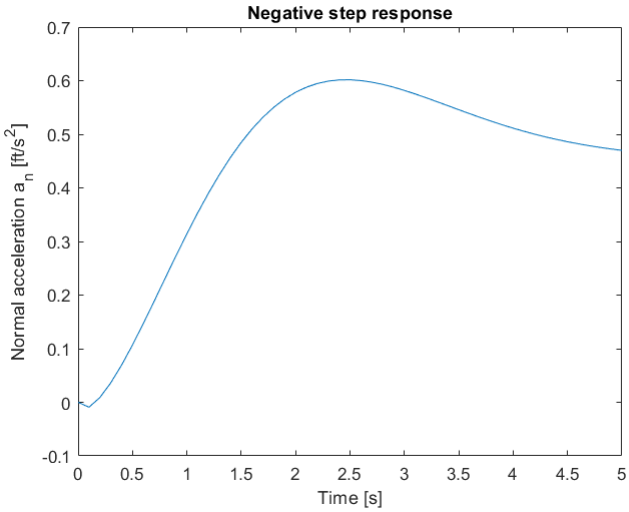

Figure 2.2: Time response to negative step input on interval 0 < t < 5

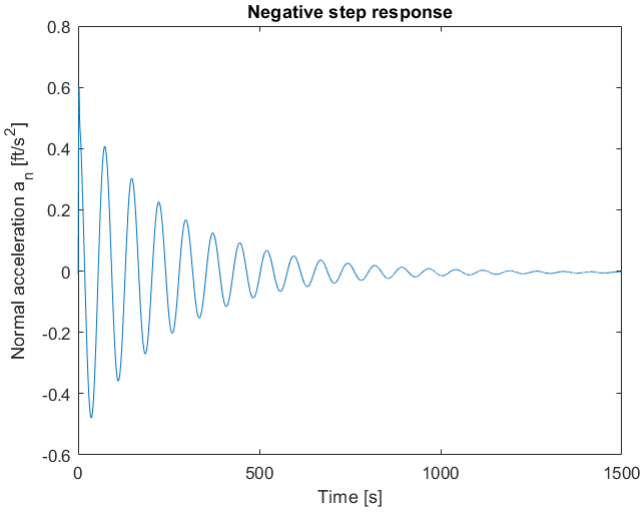

Figure 2.3: Time response to negative step input on interval 0 < t < 1000

As can be seen in Figure 2.2, the response to the negative step elevator input is not immediately upwards, but rather dips down a little before shooting up. This non-minimum phase behaviour can be explained by the zero in the right-hand side of the root-locus plot due to the gain $1/g_D$.

A physical explanation would be that due to the elevator getting an instantaneous step input, deflecting upwards, lift on the horizontal stabiliser suddenly decreases. This sudden decrease in lift causes the aircraft to 'fall' a short distance, creating negative normal acceleration, before the aircraft dynamics pick up on the subsequent increasing angle of attack lifting the plane up again.

To investigate the best accelerometer position, a plot will be made of this negative step input response for different accelerometer positions. The positions that were investigated are for x_a equals 0 ft, 5 ft,

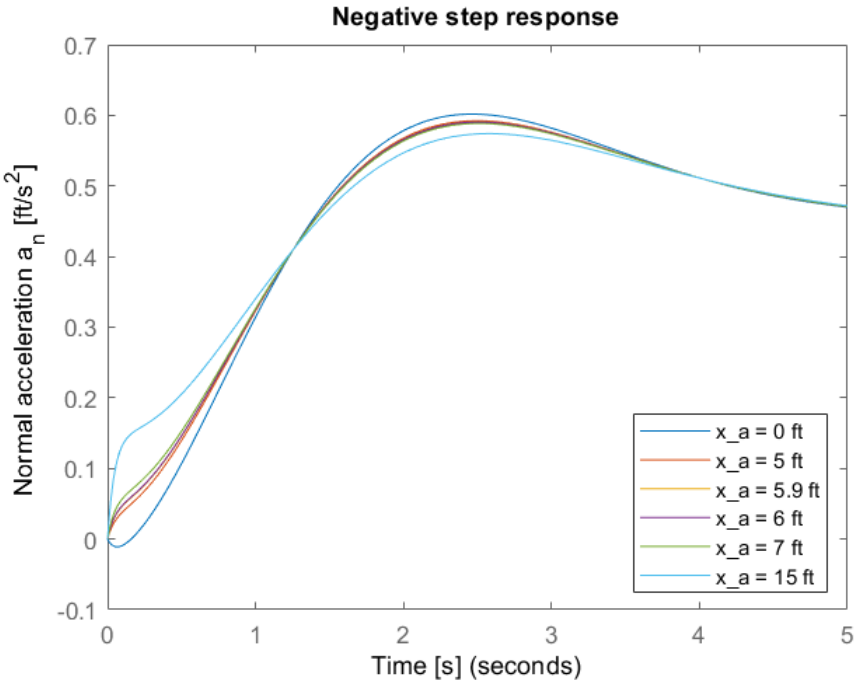

Figure 2.4: Plot of the system response to negative step input for different x_a on interval 0 < t < 5 s.

5.9 ft, 6 ft, 7 ft and 15 ft and the plot can be found in Figure 2.4 for the 5-second time response and Figure 2.5. The plot for x_a equals 0 ft in Figure 2.4 and 2.5 is the same as Figure 2.2.

The zeros for these transfer functions can be determined by the `zero(tf)` command in Matlab. The zeros are presented in Table 2.4. From this table it can be deduced that the non-minimum phase behaviour only occurs for the accelerometer position of 0 ft, due to Zero 1 being in the right-hand plane. For other accelerometer positions, this zero is in the left-hand plane, indicating no non-minimum phase behaviour. This is consistent with the results shown in Figure 2.5, where undershoot only occurs for the x_a of 0 ft.

x_a pos.	**Zero 1**	**Zero 2**	**Zero 3**	**Zero 4**
0 ft.	9.7597	-5.3925	0.0094	-0.0059
5 ft.	-1.7243 + 5.1574i	-1.7243 - 5.1574i	0.0094	-0.0059
5.9 ft.	-1.4160 + 4.5914i	-1.4160 - 4.5914i	0.0094	-0.0059
6 ft.	-1.3898 + 4.5392i	-1.3898 - 4.5392i	0.0094	-0.0059
7 ft.	-1.1840 + 4.0993i	-1.1840 - 4.0993i	0.0094	-0.0059
15 ft.	-0.6597 + 2.5969i	-0.6597 - 2.5969i	0.0094	-0.0059

Table 2.4: Zeros of the transfer function a_n/δ_e for different x_a

2.3.1. Instantaneous center of rotation

From the results presented above, a conclusion can be drawn about the instantaneous center of rotation and pilot position. The instantaneous center of rotation is the location where the rotation due to the elevator input itself does not create an initial acceleration 'bump'. From Figure 2.5, it is evident that this is true of a location x_a between 0 and 5 ft., just before 5 ft. This is the location where the first zero is in the left-hand plane and assumes the largest absolute real value.

For pilot intuition, the most beneficial location of the pilot's seat should be in or before the instantaneous center of rotation. Placing the pilot's seat in the instantaneous center of rotation ensures that during rotations, the pilot will not sense accelerations, and the accelerations will not give the pilot a false sense of movement (such as in the x_a 0 ft. case). In the case the pilot's seat is positioned before the instanta-

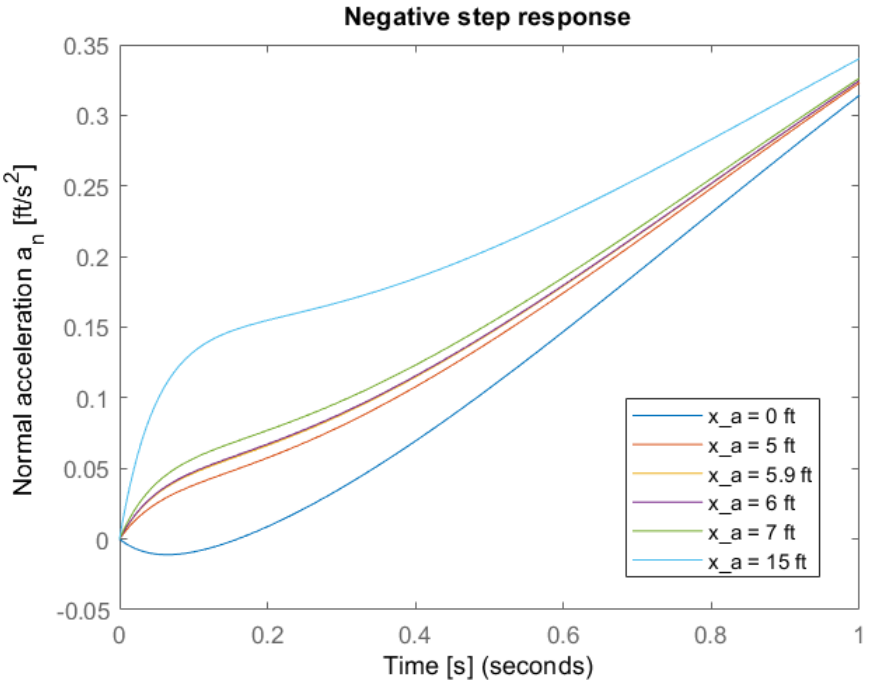

Figure 2.5: Plot of the system response to negative step input for different x_α on interval 0 < t < 1 s.

neous center of rotation, the pilot will experience a 'dropback' effect in the pitch-up manoeuvre, which is still preferable to the the overshoot effect.

One other aspect to consider is material stiffness and bending deformation in the aircraft's structure as sharp turns are taken. Bending can cause a slight delay for the accelerations involved to take effect, resulting in false accelerations that are only affecting the specific part of the aircraft the sensor is located, as opposed to the accelerations affecting the entire system. To negate this effect, the sensor should be placed in or as close as possible to the neutral point (node) of the most prominent bending mode of the fuselage.

3

Open Loop Analysis

In this chapter the LTI model used in the last chapter is reduced and the state space for the lateral and longitudinal motions are determined for the specific flight condition. The altitude used is $20,000\ ft$ and velocity of $600\ ft/s$, as indicated in Table 2.1.

3.1. State Space determination

First of all , the LTI model is reduced which contains 18 states. The model has to be reduced to two separate systems which contain both the longitudinal and lateral dynamics respectively. The states that will be included are as follow:

- **Longitudinal states :** V, α, θ, q
- **Lateral States :** β, ϕ, p, r

3.2. Longitudinal Model

The longitudinal model is obtained by reducing the $A_{longitudelo}$ matrix obtained from the low fidelity model. Once the matrix is obtained the longitudinal state space vectors A_{lon} & $B_{lon}$are obtained by simple row reduction of the $6x6$ matrix. The matrix representation is shown below.

$$A_{lon} = \begin{bmatrix} -0.0109 & -1.7611 & -32.1700 & -0.8207 \\ -0.0002 & -0.6505 & 0.0000 & 0.9482 \\ 0 & 0 & 0 & 1.0000 \\ -0.0000 & -1.9092 & 0 & -0.8893 \end{bmatrix} \tag{3.1}$$

$$B_{lon} = \begin{bmatrix} 0.0016 & 0.1093 \\ 0 & -0.0014 \\ 0 & 0 \\ 0 & -0.1389 \end{bmatrix} \tag{3.2}$$

The resulting state-space system will have the form :

$$\begin{bmatrix} \dot{V} \\ \dot{\alpha} \\ \dot{\theta} \\ \dot{q} \end{bmatrix} = \begin{bmatrix} -0.0109 & -1.7611 & -32.1700 & -0.8207 \\ -0.0002 & -0.6505 & 0.0000 & 0.9482 \\ 0 & 0 & 0 & 1.0000 \\ -0.0000 & -1.9092 & 0 & -0.8893 \end{bmatrix} \begin{bmatrix} V \\ \alpha \\ \theta \\ q \end{bmatrix} + \begin{bmatrix} 0.0016 & 0.1093 \\ 0 & -0.0014 \\ 0 & 0 \\ 0 & -0.1389 \end{bmatrix} \begin{bmatrix} \delta_t \\ \delta_e \end{bmatrix} \tag{3.3}$$

The longitudinal model gives the output for the longitudinal motions , phugoid and short period motions.

3.3. Lateral Model

The lateral model is obtained by reducing the matrix $A_{lateral lo}$ obtained by running the low fidelity model under the given flight conditions. Once the matrix is obtained it is reduced to the lateral state space vectors A_{lat} & B_{lat} by simple row and column reduction. The lateral state vectors are as follows:

$$A_{lat} = \begin{bmatrix} -0.2055 & 0.0535 & 0.0594 & -0.9941 \\ 0 & 0 & 1.0000 & 0.0595 \\ -25.8584 & 0 & -2.3166 & 0.4924 \\ 7.2786 & 0 & -0.0294 & -0.3191 \end{bmatrix} \tag{3.4}$$

$$B_{lat} = \begin{bmatrix} 0.0002 & 0.0005 \\ 0 & 0 \\ -0.5576 & 0.0755 \\ -0.0309 & -0.0571 \end{bmatrix} \tag{3.5}$$

The resulting state-space system will have the form :

$$\begin{bmatrix} \dot{\beta} \\ \dot{\phi} \\ \dot{p} \\ \dot{r} \end{bmatrix} = \begin{bmatrix} -0.2055 & 0.0535 & 0.0594 & -0.9941 \\ 0 & 0 & 1.0000 & 0.0595 \\ -25.8584 & 0 & -2.3166 & 0.4924 \\ 7.2786 & 0 & -0.0294 & -0.3191 \end{bmatrix} \begin{bmatrix} \beta \\ \phi \\ p \\ r \end{bmatrix} + \begin{bmatrix} 0.0002 & 0.0005 \\ 0 & 0 \\ -0.5576 & 0.0755 \\ -0.0309 & -0.0571 \end{bmatrix} \begin{bmatrix} \delta_a \\ \delta_r \end{bmatrix} \tag{3.6}$$

The lateral motions , dutch roll , spiral stability and aperiodic roll are obtained from the this model.

3.4. Eigenmotion Characteristics

The eigenmotions are calculated by determining the eigen values of matrices A_{lon} &A_{lat} respectively. The eigen values of both the matrices are given as follows:

Longitudinal Eigen Values[2]	Lateral Eigen Values
-0.7713 + 1.3392i	-0.3083 + 2.9290i
-0.7713 - 1.3392i	-0.3083 - 2.9290i
-0.0040 + 0.0675i	-2.2146 + 0.0000i
-0.0040 - 0.0675i	-0.0101 + 0.0000i

Table 3.1: Lists of eigen values

The eigenmotion characteristics can be calculated by means of the given equations :

$$\omega_0 = \sqrt{Re(\lambda)^2 + Im(\lambda)^2} \tag{3.7}$$

$$\zeta = \frac{-Re(\lambda)}{\omega_0} \tag{3.8}$$

$$P = \frac{2\pi}{Im(\lambda)} \tag{3.9}$$

$$T_{1/2} = \frac{-ln(2)}{Re(\lambda)} \tag{3.10}$$

3.4.1. Periodic Motions

The periodic motions are obtained from the eigen values of the A_{lon} matrix which contains the longitudinal modes. And the eigen values of the dutch roll which is also periodic in nature is obtained from A_{lat}. The eigen values having a low natural frequency belongs to the phugoid motion. The values having higher natural frequency belongs to the short period. From these values the eigen motion characteristics are determined. The characteristics and the motions related to the phugoid and short period along with the time response graphs are shown below.

Modes	Eigenvalues	ω_n	ζ	P	$T_{\frac{1}{2}}$
Phugoid	-0.0040 ±0.0675i	0.0676	0.0588	93.1239	174.5140
Short period	-0.7713 ±1.3392i	1.5454	0.4991	4.6918	0.8986
Dutch roll	-0.3083 ±2.9290i	2.9452	4.5610	2.1452	2.2485

Table 3.2: Periodic Motions

Looking at the characteristics of the periodic motions, it can be seen that the real part of each motion is negative. Meaning all motions are inherently stable. Furthermore, the motions are damped enough to sustain a controllable flight environment. A more in dept analysis of each motion is shown below. With graphs for each relevant flight variable.

Figure 3.1 shows the time response of the phugoid motion, which is the result of a downward elevator deflection of > 3s. This results in the aircraft pitching downwards, decreasing the angle of attack and increasing the velocity.

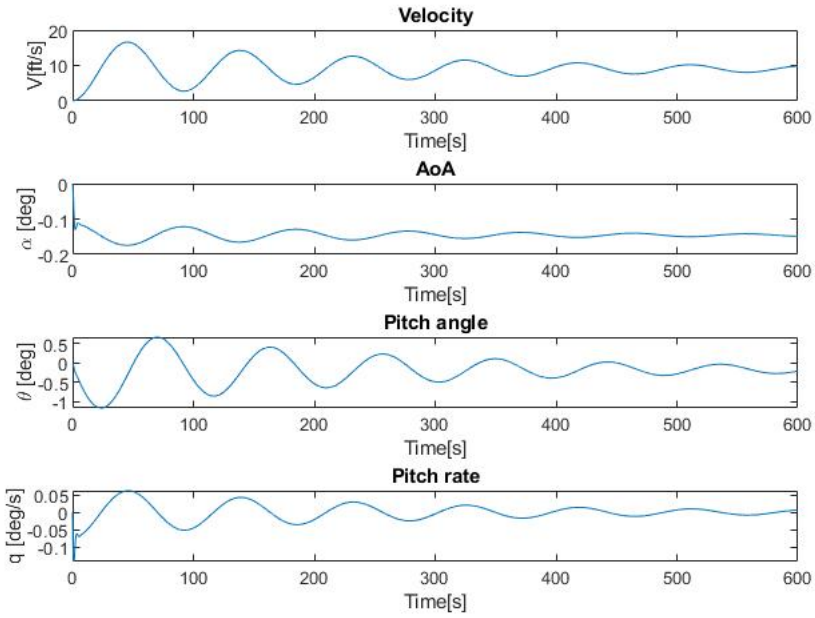

Figure 3.1: Phugoid Motion Time Response

From the graphs, it can be seen that this motion oscillates but is quickly damped out back to steady horizontal flight.

The short period, which is very similar to the Phugoid motion also results from a downward elevator deflection, however this input should be < 1s. The velocity and angle of attack should remain roughly the same, while the main attention point would be the pitch angle and pitch rate.

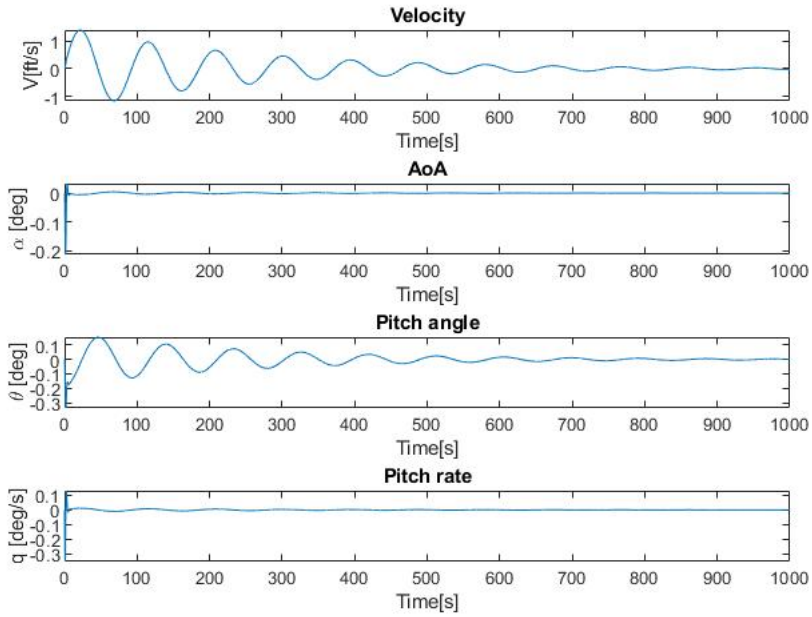

Figure 3.2: Short Period Time Response

The Dutch roll is induced by deflecting the rudder. Providing a lateral eigenmotion causing a yawing and then rolling motion. The result of this can be seen in Figure 3.3.

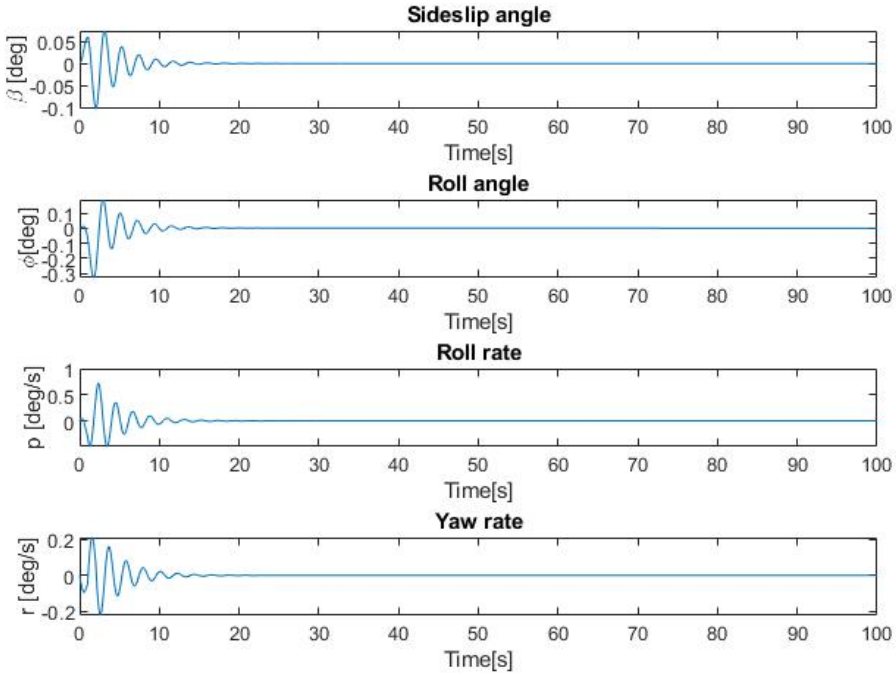

Figure 3.3: Dutch Roll Time Response

As can be seen from the graph and the values in Table 3.3. The Dutch roll motion is the most heavily

damped motion. Steady horizontal flight is achieved at less then 20 seconds

3.4.2. Aperiodic Motions

The aperiodic motions include the aperiodic roll and the spiral stabilty whihc are the lateral modes. The eigen values for both of these can be obtained from the matrix A_{lat}.The eigen motion characteristics are determined from these respective eigen values. The eigenmotion characteristics along woth the time responses are shown below for both aperiodic roll and spiral stability.

Modes	Eigen Values	ω_n	τ	$T_{\frac{1}{2}}$
Aperiodic Roll	-2.2146 + 0.0000i	2.2146	0.4514	0.3130
Spiral Stability	-0.0101 + 0.0000i	0.0101	99.1889	68.7525

Table 3.3: Aperiodic Motions

Similar as to the periodic motions, the real part of both aperiodic modes are negative, meaning both motions are stable. A more in dept analysis of eah motion is shown below.

Figure 3.4 shows the motion of the aperiodic roll, which is induced by the deflection of the aileron control surface. This results in a rolling moment which is then damped by the difference in lift due to the upward or downward motion of the wings.

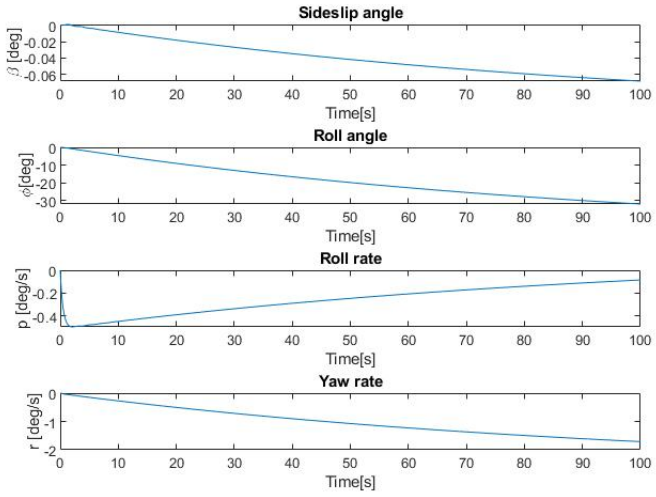

Figure 3.4: Aperiodic Roll Time Response

From the graphs it can be seen that the motion is stable but the path of the aircraft does not return to a horizontal flight. Therefore, a small correction has to be made after inducing this motion.

The last motion is the Spiral, shown in Figure 3.5, which is induced by maintaining a certain roll angle for < 3s. Due to this, the aircraft will start rolling and yawing. In this case the motion is stable, which is not true for all aircraft. Similar to the Aperiodic roll, the motion does not return to horizontal flight and will need to be corrected.

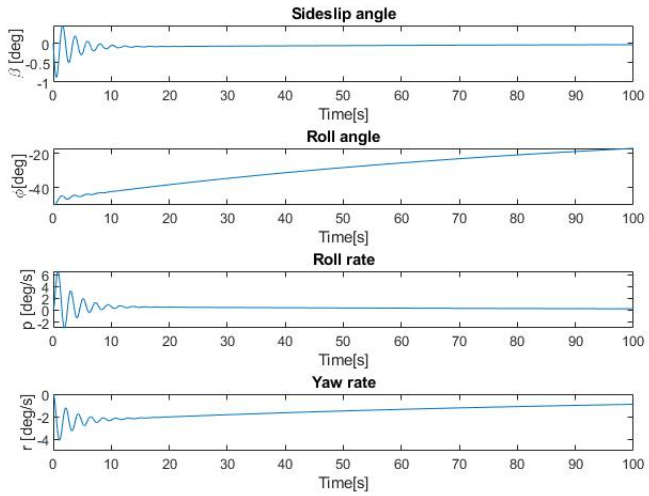

Figure 3.5: Spiral Stability Time Response

4

Design of the pitch rate command system

In this chapter the designing of the pitch rate command system is discussed.The command system is effective for tracking tasks at low velocities. The designed pitch rate controller has to meet the requirements of the CAP and Gibson criterion.The design and verification process is discussed in details below. The altitude used is $20,000ft$ and velocity is $600ft/s$ as indicated in Table 2.1

4.1. Reduced short period model

Earlier the longitudinal states were obtained from the matrix $A_{longitudelo}$. The longitudinal state matrix that contains both the phugoid and short period motion is A_{lon}(**??**) and the matrix B_{lon}(**??**) has the inputs.. The A matrix for the short period is obtained by extracting the 2^{nd} and 4^{th} columns and rows respectively from the A_{lon} matrix. The B matrix is obtained similarly from the B_{lon} matrix by extracting the 2^{nd} column and 2^{nd} and 4^{th} rows respectively. The resulting A and B matrices for the short period motion are as follows :

$$A_{short\ period} = \begin{bmatrix} -0.6505 & 0.9482 \\ -1.9092 & -0.8893 \end{bmatrix} \tag{4.1}$$

$$B_{short\ period} = \begin{bmatrix} -0.0014 \\ -0.1389 \end{bmatrix} \tag{4.2}$$

The state vectors are :

$$x = \begin{bmatrix} \alpha \\ q \end{bmatrix} \tag{4.3}$$

The resulting matrix equation can be written as:

$$\begin{bmatrix} \dot{\alpha} \\ \dot{q} \end{bmatrix} = \begin{bmatrix} -0.6505 & 0.9482 \\ -1.9092 & -0.8893 \end{bmatrix} \begin{bmatrix} \alpha \\ q \end{bmatrix} + \begin{bmatrix} -0.0014 \\ -0.1389 \end{bmatrix} \delta_e \tag{4.4}$$

The C matrix is chosen as an identity matrix of $2x2$ and the D matrix of the state space is a null vector.

$$C_{short\ period} = \begin{bmatrix} 1 & 0 \\ 0 & 1 \end{bmatrix} \tag{4.5}$$

$$D_{short\ period} = [0] \tag{4.6}$$

The 4 state system is made from the initial state space matrices from Ch.3 . The 2 state system is constructed using the reduced short period matrices. The short period motion for both the systems are visualised below. For the initial response in Figure4.1 it can be notice that the short period motion is dominant for both the systems. However over prolonged time , it can be noticed that the 4 state model shows a prolonged phugoid response where the 2-state model does not show any such behavior and it

stabilises. The reason behind this that the 4-state model has the velocity V included in it and the 2 state model lack the velocity. For designing, the 2 state model can be used as it shows similar behaviour the 4 state model in terms of short period at the initial stage as only short term response is used.

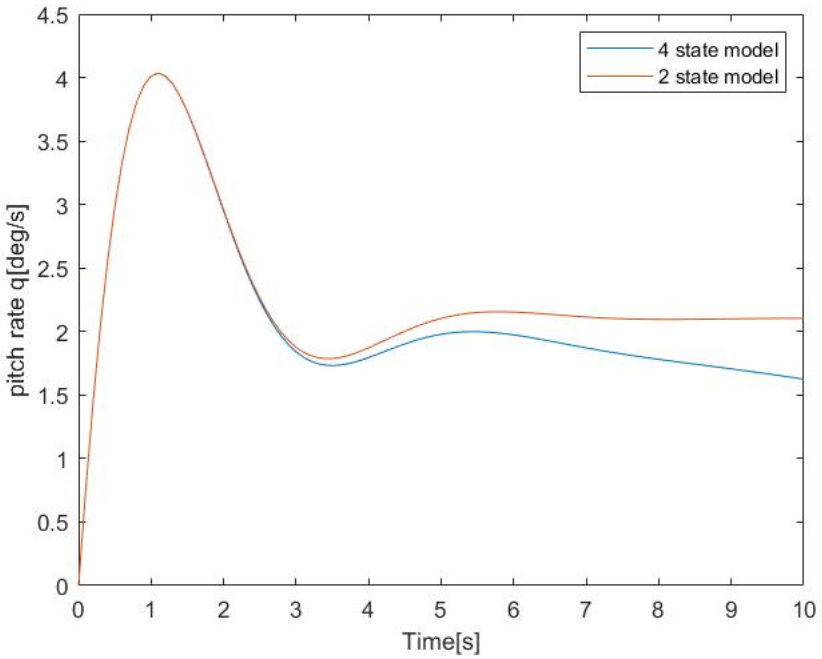

Figure 4.1: Initial pitch rate time response to a elevator step input

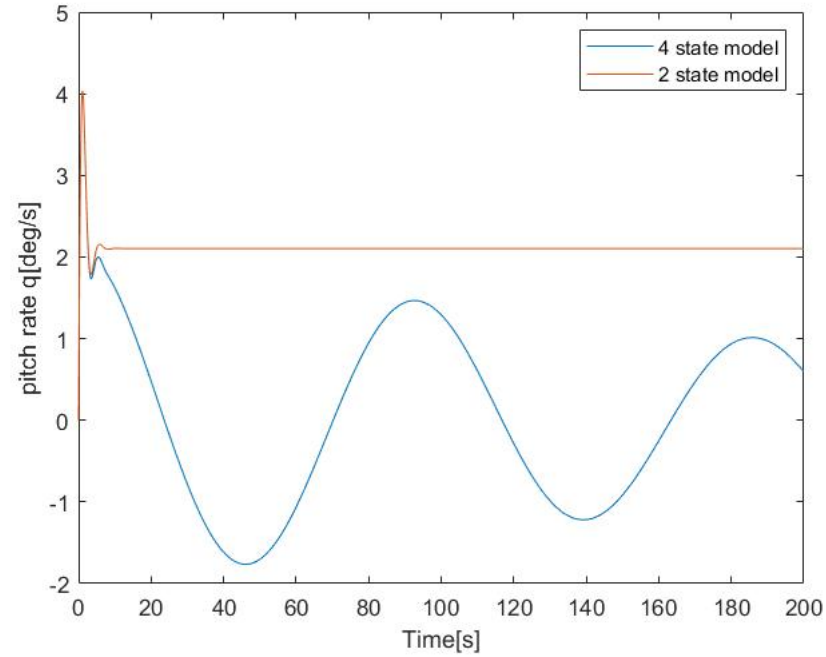

Figure 4.2: Time pitch rate response to a elevator step input

4.2. Determination of poles and gains

To determine the poles and gain and also to satisfy the CAP and Gibson criterion , the requirements are to be converted into the frequency domain. The conversion can be done by implementing the formulas mentioned in van Kampen, 2020:

$$\omega_{n_{sp}}(V,h) = 0.03V(V,h) \tag{4.7}$$

$$\zeta_{sp}(V,h) = 0.5 \tag{4.8}$$

$$T_{\theta_2}(V,h) = \frac{1}{0.75w_{n_{sp}}} \tag{4.9}$$

For the chosen flight condition the velocity V is $182.88m/s$ which givies the following:

$$\omega_{n_{sp}} = 5.4864rad/s \tag{4.10}$$

$$T_{\theta_2} = 0.2430s \tag{4.11}$$

The poles can be determined from the roots of the 2^{nd} order equation given below:

$$s^3 + 2\omega_{n_{sp}}\zeta_{sp}s + \omega_{n_{sp}}^2 = 0 \tag{4.12}$$

The roots are as follows :

$$p_1, p_2 = \omega_{n_{sp}}\zeta_{sp} \pm \omega_{n_{sp}}\sqrt{\zeta_{sp}^2 - 1} \tag{4.13}$$

$$= -2.7432 \pm 4.7514i \tag{4.14}$$

The MATLAB build-in function *'place'* is used to determine the gains for angloe of attack α and pitch rate q respectively , which are:

$$\begin{aligned} K_a &= -190.9868°/rad \\ K_q &= -26.5239°/rad/s \end{aligned} \tag{4.15}$$

In order to check whether the gains are acceptable, a response to the vertical gust is taken. The vertical gust velocity is taken as $4.572m/s$. From there the induced angle of attack , $\alpha_{induced}$ can be determined and also the elevator deflection δ_e due to it. The values of both the parameters are given below:

$$\alpha_{induced} = \arctan(\frac{v_{gust}}{V}) = \arctan(\frac{4.572}{182.88}) = 0.0250rad \tag{4.16}$$

$$\delta_{e_{induced}} = K_a\alpha_{induced} = -4.7737° \tag{4.17}$$

The elevator delfection due to vertical gust falls in range of the allowable deflection as it is below $-25°$.

4.3. Lead Lag filter

Once the poles are calculated to achieve the desired frequency and damping for the short period , a lead- lag filter is used to get the desired $\omega_{n_{sp}}$. The equation of the lead lag filter is given by :

$$G_{prefilter} = \frac{1 + T_{\theta_2}s}{1 + T_{\theta_{2old}}s} \tag{4.18}$$

The value of $T_{\theta_{2old}}$ is calculated by taking the frequency value of short period from the original model. Similarly the pitch rate to elevator transfer function can also be determined using the following:

$$\frac{q}{\delta_e} = K_q\frac{T_{\theta_{2old}s+1}}{s^2 + \omega_{sp} + \omega sp^2} \tag{4.19}$$

Finally by using the obtained values the transfer functions can be obtained for the lead lag filter as:

$$G_{prefilter} = \frac{0.243s + 1}{0.8628s + 1} \tag{4.20}$$

And that of the pitch rate to elevator as :

$$\frac{q}{\delta_e} = \frac{-22.88s - 26.52}{s^2 + 5.486s + 30.1} \tag{4.21}$$

The lead lag filter is kept outside the feedback loop so that it does not effect the original system dynamics and the desired frequency and damping ration can be calculated.

4.4. Verification of CAP and Gibson criterion

To determine whether the sysmtem fulfills the requirements, the value for CAP and dropback criteria are to be calculated. The values can be obtained from the following expressions,

$$CAP = \frac{g\omega_{n_{sp}}^2 T_{\theta_2}}{V} \tag{4.22}$$

$$\frac{DB}{q_{ss}} = T_{\theta_2} - \frac{2\zeta_{sp}}{\omega_{n_{sp}}} \tag{4.23}$$

The values for the 4 state model and 2 state reduced short period model are diplayed in the table below:

Values	**CAP**	**Gibson criteria**
4 state model	0.1105	0.6808
2 state model	0.3924	0.0608

Table 4.1: CAP and Gibson criteria values for the original and reduced models respectively

To verify the Gibson Mil specs , at first a pitch rate and pitch angle response is plotted for a step input which can be used to determine the pitch rate overshoot ratio.From the image **??** the pitch rate overshoot($\frac{q_m}{q_s}$) can be estimated around 1.22.From the image 4.5 it can be easily concluded that the drop-back rate is inside the satisfactory levels.In image 4.6 the CAP vs short damping ratio for both the 2 state reduced model and 4 state models are compared. It is to be noted that even though the model is reduced the value of CAP for the 2 state model lies withing the Level 1 requirement of CAP for all the flight phases.

Evaluation Group	Trial 1	Trial 2	Trial 3	…	Trial n
1	A1	A2	A3	…	An
2	A1	A2	A3	…	An
3	A1	A2	A3	…	An
□	□	□	□	□	□
10	A1	A2	A3	…	An

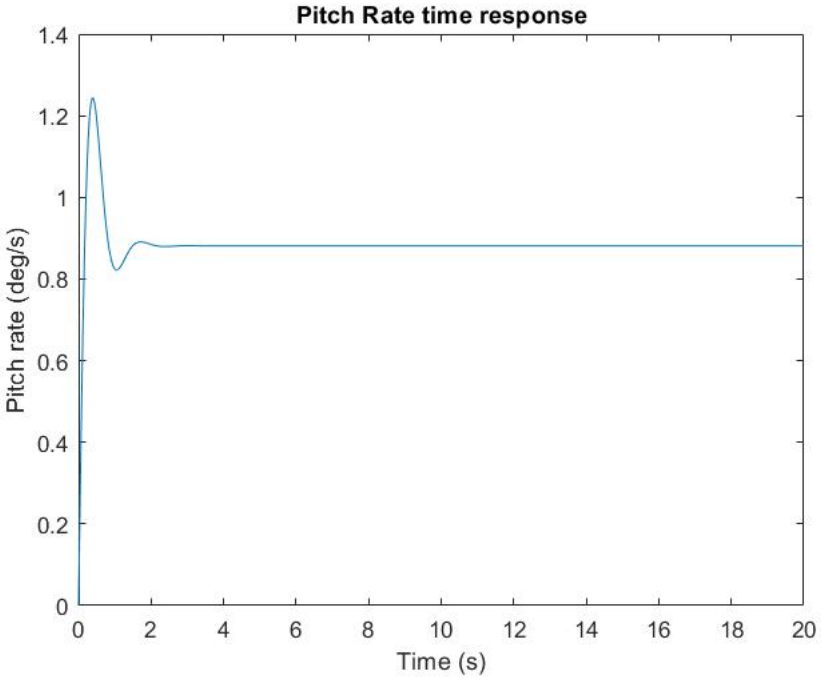

Figure 4.3: Time response of pitch rate to a step input

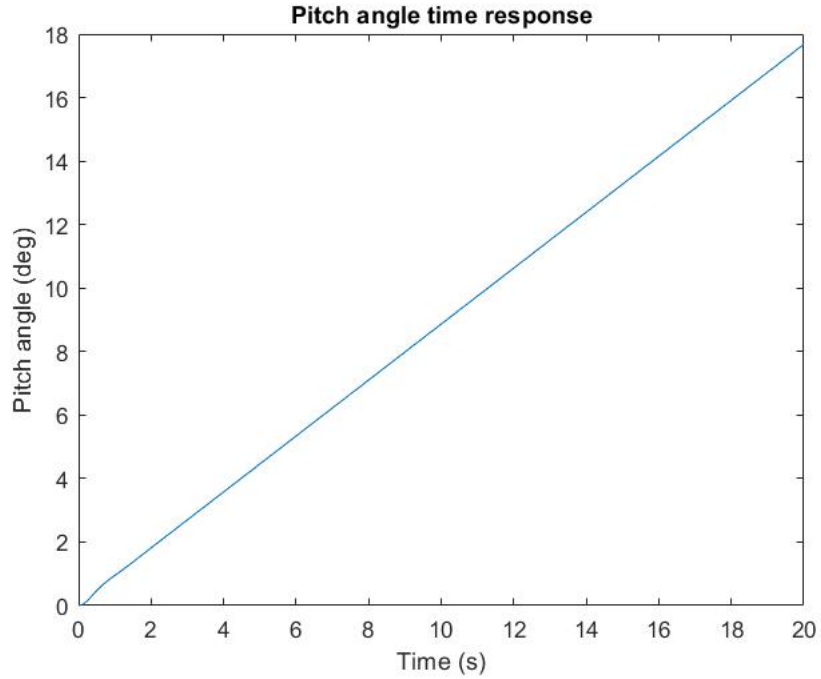

Figure 4.4: Time response of pitch angle to a step input

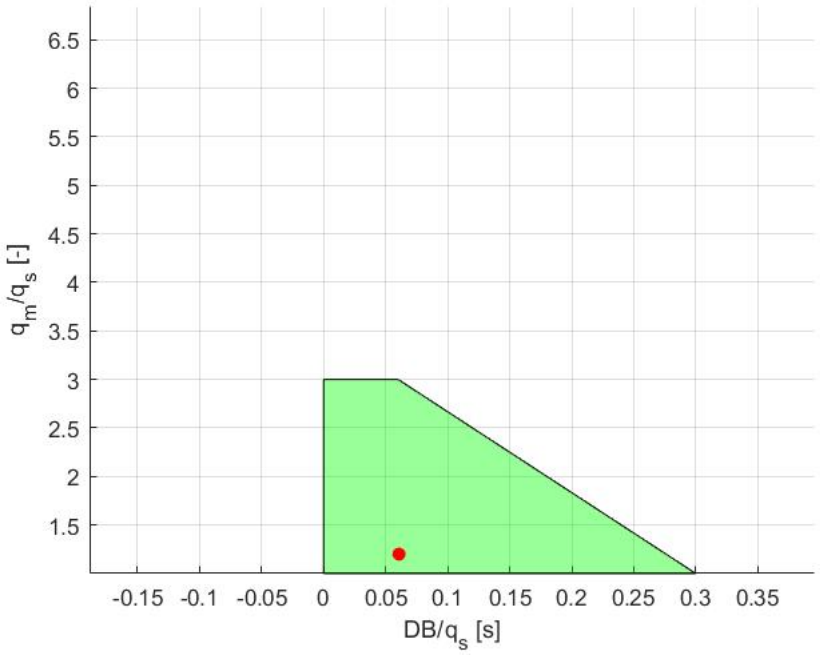

Figure 4.5: Verification of the Gibson criteria for the reduced model

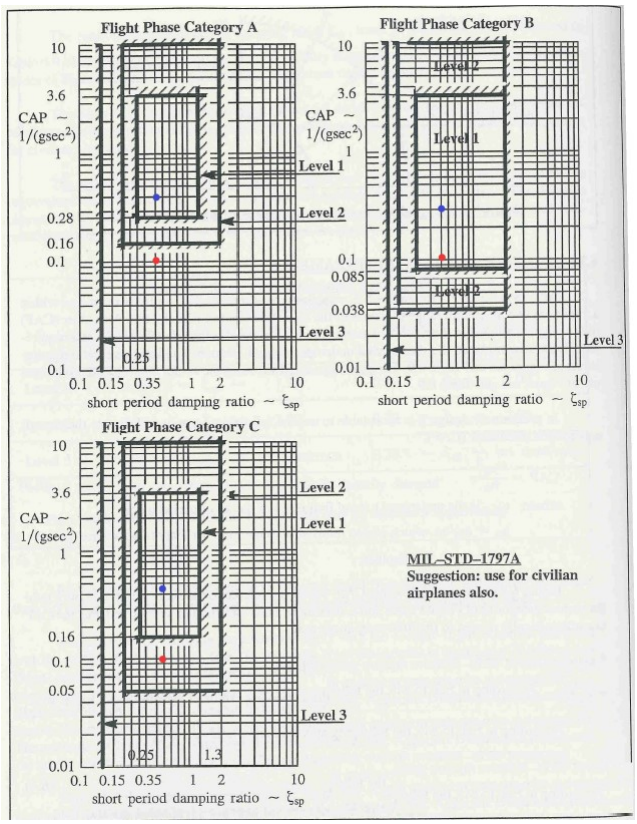

Figure 4.6: Verification of the CAP for the reduced model(blue) , 4state model(red)

5

Design of the glideslope and flare controller systems

For the final part of the assignment, an automatic landing system is designed. The automatic landing system is in fact a combination of three subsystems, the glideslope follower, the localizer and the automatic flare controller. In this chapter, only the longitudinal modes are considered, omitting the localizer. The glideslope follower is a control system that follows the glideslope plane by pitching up when under it and pitching down when over it. The automatic flare controller is a system that automatically pulls up the aircraft's nose just before touchdown, to lower its vertical speed such that the impact is not too heavy. Additionally, this flare manoeuvre helps the aircraft bleed off even more speed.

5.1. Problem Geometry

The simulation to test if the glideslope follower and localizer work correctly is as shown in Figure 5.1. Due to model constraints, the airport will be considered to be located at 3000 ft altitude and the landing will be commenced at 300 ft/s and 5000 ft altitude. After start of the simulation, the aircraft will remain in straight, wings level flight for about 10 seconds before starting descent. The glideslope is fixed at 3° and the simulation stops upon touchdown. è

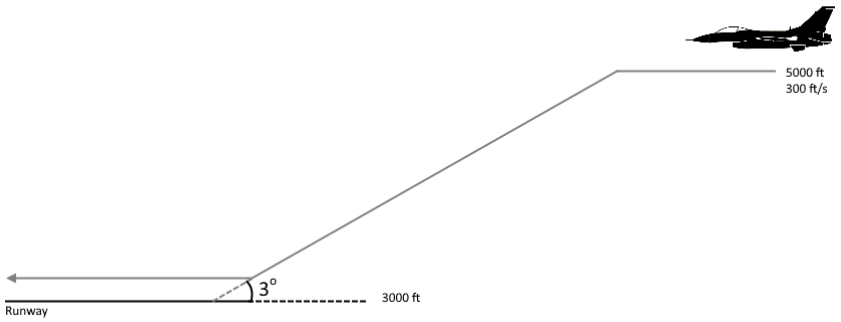

Figure 5.1: Schematic of the simulation geometry

5.2. Model reduction

In order to design the glideslope follower and flare controller, the F16 model is trimmed and linearised in the same manner as in previous chapters (note the different altitude and speed). The cost function values are given in Table 5.1 to verify the validity of the trim and linearisation.

Low-Fi	High-Fi
4.7464e-30	7.8918e-06

Table 5.1: Cost function values of the landing system trim and linearisation.

Since both of these autopilot modes are longitudinal, the model will be reduced to include the longitudinal states altitude h, true airspeed V_t, angle of attack α, pitch angle θ and pitch rate q. This reduction yields the A, B, C and D matrices presented in Equation 5.1, 5.2, 5.3 and 5.4.

$$A_{reduced} = \begin{bmatrix} 0 & 0 & -300.00 & 300.00 & 0 \\ 1.3165e-4 & -2.9097e-2 & 2.1300 & -32.170 & -2.8952 \\ 3.1537e-6 & -6.9700e-4 & -5.4466e-1 & 4.5498e-13 & 9.1522e-1 \\ 0 & 0 & 0 & 0 & 1 \\ -4.6987e-21 & 1.0385e-18 & 3.3032e-1 & 0 & -8.1694e-1 \end{bmatrix} \tag{5.1}$$

$$B_{reduced} = \begin{bmatrix} 0 & 0 \\ 1.5440e-3 & -4.5338e-3 \\ -9.4931e-07 & -1.1164e-3 \\ 0 & 0 \\ 0 & -5.7016e-2 \end{bmatrix} \tag{5.2}$$

$$C_{reduced} = \begin{bmatrix} 1.0 & 0 & 0 & 0 & 0 \\ 0 & 1.0 & 0 & 0 & 0 \\ 0 & 0 & 57.296 & 0 & 0 \\ 0 & 0 & 0 & 57.296 & 0 \\ 0 & 0 & 0 & 0 & 57.296 \end{bmatrix} \tag{5.3}$$

$$D_{reduced} = \begin{bmatrix} 0 & 0 \\ 0 & 0 \\ 0 & 0 \\ 0 & 0 \\ 0 & 0 \end{bmatrix} \tag{5.4}$$

With these matrices, the state space system serving as the aircraft model can be constructed.

5.3. Controller design

The glideslope and flare controllers were designed according to the block diagrams shown in the slides.

5.3.1. Model setup

5.3.2. Simulation model

5.3.3. Simulation results

6

Conclusion

Bibliography

Russell, R. S. (2003). Non-linear f-16 simulation using simulink and matlab.

van Kampen, E. (2020). Practical assignment ae4-301p: Exercise automatic flight control system design.